Highly Luminescent Silicon Nanocrystals with Discrete Optical Transitions

Justin D. Holmes,† Kirk J. Ziegler, R. Christopher Doty, Lindsay E. Pell, Keith P. Johnston, and Brian A. Korgel*

Contribution from the Center for Nano- and Molecular Science and Technology, Department of Chemical Engineering and Texas Materials Institute, University of Texas, Austin, Texas 78712

Received August 8, 2000. Revised Manuscript Received February 16, 2001

Abstract: A new synthetic method was developed to produce robust, highly crystalline, organic-monolayer passivated silicon (Si) nanocrystals in a supercritical fluid. By thermally degrading the Si precursor, diphenylsilane, in the presence of octanol at 500 °C and 345 bar, relatively size-monodisperse sterically stabilized Si nanocrystals ranging from 15 to 40 Å in diameter could be obtained in significant quantities. Octanol binds to the Si nanocrystal surface through an alkoxide linkage and provides steric stabilization through the hydrocarbon chain. The absorbance and photoluminescence excitation (PLE) spectra of the nanocrystals exhibit a significant blue shift in optical properties from the bulk band gap energy of 1.2 eV due to quantum confinement effects. The stable Si clusters show efficient blue (15 Å) or green (25−40 Å) band-edge photoemission with luminescence quantum yields up to 23% at room temperature, and electronic structure characteristic of a predominantly indirect transition, despite the extremely small particle size. The smallest nanocrystals, 15 Å in diameter, exhibit discrete optical transitions, characteristic of quantum confinement effects for crystalline nanocrystals with a narrow size distribution.

Introduction

Semiconductor cluster properties depend on size. For example, quantum confinement effects lead to unique electronic and optical properties, such as size-tunable excitation and luminescence energies with an overall loss of energy level degeneracy.[1] By studying the discrete energetic states that appear, these clusters can provide a test of our current understanding of quantum mechanics. Examples of size-dependent discrete optical transitions exist for clusters of direct band gap semiconductors, such as CdSe[1,2] and InAs.[3] This loss of energy level degeneracy, however, has not previously been observed in the optical properties of Si nanocrystals.[4−8] Why is Si different? Figure 1 shows the Brillouin zone and band structure for bulk Si. In Si, the lowest lying Γ → X energetic transition violates conservation of momentum; therefore, light absorption requires phonon assistance, resulting in a very low transition probability.[9] Consequently, bulk Si photoluminescence is very weak. Quantum confinement in Si nanocrystals[4−8,10] and porous Si[11] leads to enhanced luminescence efficiencies with quantum yields that have reached as high as 5% at room temperature[4] and blue-shifted "band gap" energies. However,

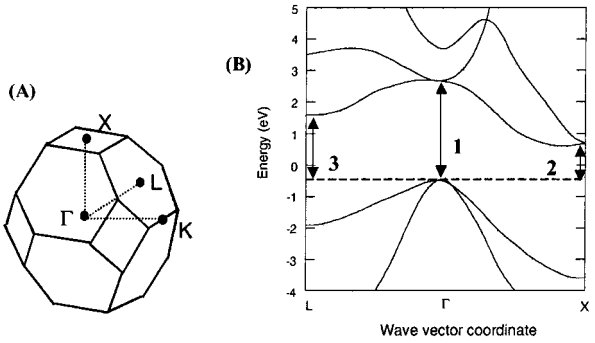

Figure 1. (A) Brillouin zone for the diamond lattice. (B) Bulk band structure for Si. The arrows indicate the energies of the direct Γ → Γ (**1**) transition, and the indirect phonon-assisted Γ → L (**3**) and Γ → X (**2**) transitions. Note that the direct transition at $k = 0$ (the Γ → Γ transition) is a saddle point. Ramakrishna and Friesner[21] predicted that the indirect transitions increase in energy with decreased quantum dot size, with a slight red-shift in the direct transition energy. This prediction arises from the qualitative difference between the parabolic conduction band structure of a direct semiconductor and the saddle-point conduction band structure of the indirect semiconductor.

* To whom correspondence should be addressed.
† Current address: Department of Chemistry, University College Cork, Cork, Ireland.

(1) For example, see: Alivisatos, A. P. *Science* **1996**, *271*, 933 and references contained therein.
(2) Murray, C. B.; Norris, D. J.; Bawendi, M. G. *J. Am. Chem. Soc.* **1993**, *115*, 8706.
(3) Banin, U.; Lee, C. J.; Guzelian, A. A.; Kadavanich, A. V.; Alivisatos, A. P.; Jaskolski, W.; Bryant, G. W.; Efros, A. L.; Rosen, M. *J. Chem. Phys.* **1998**, *109*, 2306.
(4) Wilson, W. L.; Szajowski, P. F.; Brus, L. E. *Science* **1993**, *262*, 1242. Littau, K. A.; Szajowski, P. J.; Muller, A. J.; Kortan, A. R.; Brus, L. E. *J. Phys. Chem.* **1993**, *97*, 1224. Brus, L. E.; Szajowski, P. F.; Wilson, W. L.; Harris, T. D.; Schuppler, S.; Citrin, P. H. *J. Am. Chem. Soc.* **1995**, *117*, 2915. Brus, L. *J. Phys. Chem.* **1994**, *98*, 3575.
(5) Heath, J. R. *Science* **1992**, *258*, 1131. Batson, P. E.; Heath, J. R. *Phys. Rev. Lett.* **1993**, *71*, 911.
(6) Bley, R. A.; Kauzlarich, S. M. *J. Am. Chem. Soc.* **1996**, *118*, 12461. Yang, C.-S.; Bley, R. A.; Kauzlarich, S. M.; Lee, H. W.; Delgado, G. R. *J. Am. Chem. Soc.* **1999**, *121*, 5191.
(7) Van Buuren, T.; Dinh, L. N.; Chase, L. L.; Siekhaus, W. J.; Terminello, L. J. *Phys. Rev. Lett.* **1998**, *80*, 3803.
(8) (a) Wilcoxon, J. P.; Samara, G. A. *Appl. Phys. Lett.* **1999**, *74*, 3164. (b) Wilcoxon, J. P.; Samara, G. A.; Provencio, P. N. *Phys. Rev. B* **1999**, *60*, 2704.
(9) Sze, S. M. *Physics of Semiconductor Devices*, 2nd ed.; Wiley: New York, 1981.
(10) Furukawa, S.; Miyasato, T. *Phys. Rev. B* **1988**, *38*, 5726. Takagi, H.; Ogawa, H.; Yamzaki, Y.; Ishizaki, A.; Nakagiri, T. *Appl. Phys. Lett.* **1990**, *56*, 2379.
(11) Canham, L. T. *Appl. Phys. Lett.* **1990**, *57*, 1046.

10.1021/ja002956f CCC: $20.00
Published on Web 03/28/2001

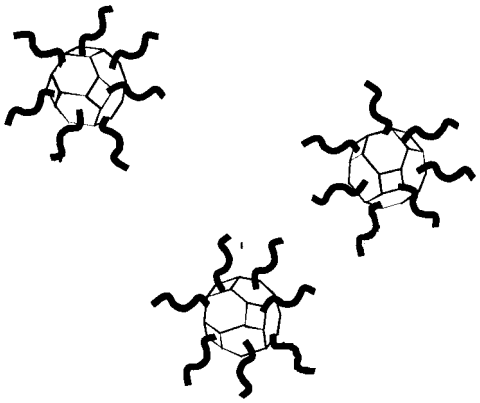

Figure 2. Illustration of sterically stabilized nanocrystals. Flexible organic molecules, such as alkanes, provide repulsive interactions between other nanocrystals in solution, thus preventing uncontrolled particle growth and aggregation. The crystalline semiconductor core tends to be well-defined and faceted.

in sharp contrast to their direct band gap semiconductor counterparts, Si nanocrystals have not displayed discrete electronic transitions in the absorbance and photoluminescence excitation (PLE) spectra.[4−8] Without experimental evidence to the contrary, one might argue that even the smallest quantum dots of Si, with its indirect band gap, will not exhibit discrete electronic transitions at room temperature due to the phonon-assisted continuum occurring across the excitation spectra. This would have important implications on the development of quantum electronic devices utilizing Si.

Nonlithographic strategies are required to create Si quantum dots with the necessary dimensions (<5 nm diameter) to exhibit quantum confinement effects at room temperature. The highly successful wet chemical techniques used to synthesize Group II-VI and III-V semiconductors have not been readily applied to Si, largely due to the high temperatures required to degrade the necessary precursors, which exceed the boiling points of available capping solvents. Furthermore, the covalent bonding of Si requires temperatures higher than the II-VI materials to achieve highly crystalline cores. Moderate progress has been made with alternative solution-phase reduction of Si salts[5−8] and aerosol[4] methods. These methods, however, have produced nanocrystals with extremely broad size distributions, which would smear any discrete size-dependent optical features in the absorbance and PLE spectra. Furthermore, the aerosol methods have required a thick oxide coating to stabilize their structure,[4] which has been shown recently to significantly affect the photoluminescence (PL) energies of porous Si.[12] Recently, we demonstrated that nanocrystal steric stabilization in a supercritical solvent is possible.[13] Here, we demonstrate that by using a Si surface-passivating solvent heated and pressurized above its critical point, the necessary temperatures can be reached to degrade the Si precursor while maintaining solvation of the capping ligand to arrest particle growth (Figure 2), thus combining the best assets of both the aerosol and wet chemical approaches. The high temperature of 500 °C promotes Si crystallization. The additional advantage of using a supercritical (sc) solvent over a conventional solvent is the high diffusion coefficient, on the order of 10^{-3} to 10^{-4} cm^2 s^{-1},[14] enabling

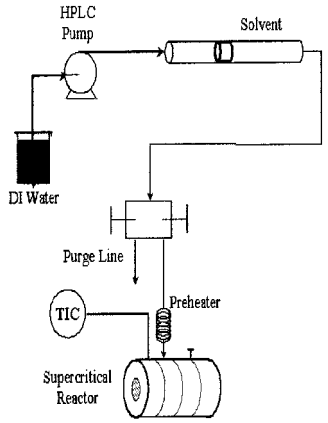

Figure 3. Schematic of the supercritical reaction apparatus used in the batch production of Si nanocrystals.

the rapid reactant diffusion necessary to achieve diffusion-limited growth for the narrowest particle size distributions possible.[15] Using this method, relatively size-monodisperse, highly stable Si nanocrystals ranging from 15 to 40 Å in diameter are produced.

This article presents the structural, chemical, and optical characterization of the Si nanocrystals produced using this method, with transmission electron microscopy (TEM), energy-dispersive X-ray spectroscopy (EDS), Fourier transform infrared spectroscopy (FTIR), UV−visible absorbance, and luminescence (both PL and PLE) spectroscopy data. The Si nanocrystals consist of crystalline cores coated by hydrocarbon ligands bound through covalent alkoxide bonds with the nanocrystal surface. The nanocrystals luminesce with size-tunable color, from the blue (15 Å diameter) to the green (25−40 Å diameter). Discrete optical transitions also appear in the absorbance and PLE spectra of the 15 Å diameter nanocrystals, which is consistent with quantum confinement effects in semiconductors.

Experimental Section

Diphenylsilane and anhydrous 1-octanol and hexane, packaged under nitrogen, were obtained from Aldrich Chemical Co. (St. Louis, MO) and stored in a nitrogen glovebox.

Organic-passivated Si nanocrystals were prepared by thermally degrading diphenylsilane in mixtures of octanol and hexane (octanol: $T_c = 385$ °C, $P_c = 34.5$ bar; hexane: $T_c = 235$ °C, $P_c = 30$ bar) well above the critical point at 500 °C and 345 bar in an inconnell high-pressure cell as shown in Figure 3. The presence of Si particles was observed by the formation of a yellow solution; no color change was observed in the absence of diphenylsilane. When diphenylsilane was degraded in the presence of sc-ethanol rather than sc-octanol, the solution quickly turned from orange to brown and then clear as polydisperse micron-sized Si particles formed and settled on the walls of the reaction vessel.[16] This result suggests that, unlike ethanol, the bound octanol chains provide sufficient steric stabilization to prevent aggregation. The sc-octanol quenches the reaction and passivates the Si nanocrystal surface.

A typical preparation begins inside a glovebox. Diphenylsilane solution (250−500 mM in octanol) is loaded into an inconnell high-pressure cell (0.2 mL) and sealed under a nitrogen atmosphere. After removing the cell from the glovebox, it is attached via a three-way valve to a stainless steel high-pressure tube (~40 cm^3) equipped with a stainless steel piston. Deionized water is pumped into the back of

(12) Wolkin, M. V.; Jorne, J.; Fauchet, P. M.; Allan, G.; Delerue, C. *Phys. Rev. Lett.* **1999**, *82*, 197.

(13) Shah, P. S.; Holmes, J. D.; Doty, R. C.; Johnston, K. P.; Korgel, B. A. *J. Am. Chem. Soc.* **2000**, *122*, 4245.

(14) McHugh, M. A.; Krukonis, V. J. *Supercritical Fluids Extraction: Principles and Practice*, 2nd ed.; Butterworth-Heinman (Boston): Boston, MA, 1993.

(15) As diffusion-limited growth proceeds, the size distribution tightens: Reiss, H. *J. Chem. Phys.* **1951**, *19*, 482.

(16) Previous studies have used sc-alcohols as solvents in the thermal synthesis of materials. For example, homo- and heterometallic submicron sized powders of titanium dioxide and $MgAlO_4$ were synthesized from alkoxide precursors in sc-ethanol at 350 °C: Barj, M.; Bocquet, J. F.; Chor, K.; Pommier, C. *J. Mater. Sci.* **1992**, *27*, 2187.

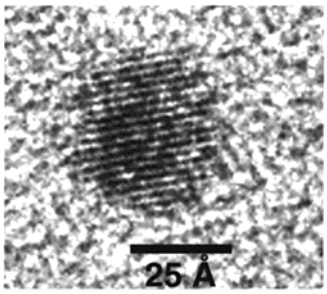

Figure 4. High-resolution TEM image of a 40 Å diameter Si nanocrystal. The lattice spacing of 3.1 Å is consistent with the (111) separation in the Si diamond-like lattice. The adsorbed organic capping layer is not visible in the TEM image. The faceted surface indicates that the nanocrystals were grown in a controlled environment.

the piston with an HPLC pump (Thermoquest) to inject oxygen-free octanol through an inlet heat exchanger and into the reaction cell to the desired pressure, between 140 and 345 bar. The cell is covered with heating tape (2 ft) and heated to 500 °C (±0.2 °C) within 15−20 min with use of a platinum resistance thermometer and a temperature controller. The reaction proceeds at these conditions for 2 h. Chloroform is used to extract the Si nanoparticles from the cell upon cooling and depressurization. The nanocrystal dispersion is subsequently dried and the organic-stabilized Si nanocrystals are redispersed in hexane or chloroform. The small 15 Å diameter particles also redisperse in ethanol. The larger Si nanocrystals, with slightly broader size distributions, are produced by increasing the Si:octanol mole ratio with hexane as a solvent; a typical Si:octanol mole ratio is 1000:1. The reaction yield in percent conversion of Si precursor to Si incorporated in the nanocrystals varies from 0.5% to 5%.

A JEOL 2010 transmission electron microscope with 1.7 Å point-to-point resolution operating with a 200 kV accelerating voltage with a GATAN digital photography system was used for transmission electron microscopy. In situ elemental analysis was performed on the nanocrystals with an Oxford energy dispersive spectrometer. Electron diffraction images were obtained with the JEOL 2010 operating at 200 kV. Absorbance spectra were recorded with a Varian Cary 500 UV-Vis-NIR spectrophotometer with Si nanocrystals dispersed in ethanol or hexane. The extinction coefficients, ϵ, were deterimined for the nanocrystals from the relationship between the measured absorbance ($A = \epsilon cl$), the path length ($l = 10$ cm), and the Si concentration determined from dry weights. The quantity ϵc is the absorption coefficient, α. Luminescence measurements were performed with a SPEX Fluorolog-3 spectrophotometer. The PL and PLE spectra were corrected with quinine sulfate as a standard. Quantum yields were calculated by comparison with 9,10-diphenylanthracene. FTIR measurements were obtained with a Perkin-Elmer Spectrum 2000 FTIR spectrometer. FTIR spectra were acquired from dried films of silicon nanocrystals deposited on Zinc Selenide windows.

Results and Discussion

Synthesis and Characterization. Figure 4 shows a TEM image of an organic-monolayer stabilized 40 Å diameter Si nanocrystal. The particle exhibits a crystalline core with a well-defined faceted surface. The lattice spacing is 3.1 Å, characteristic of the distance separating the (111) planes in diamond-like Si. Si nanocrystal formation likely propagates through a radical mechanism as shown below:[17]

$$(Ph)_2SiH_2 \rightarrow (Ph)_2SiH^{\bullet} \quad (1)$$

$$2(Ph)_2SiH^{\bullet} \rightarrow H(Ph)_2Si - Si(Ph)_2H \quad (2)$$

The benzene rings help stabilize the diphenyl silane radical intermediates by delocalizing the electron charge. These free radicals can react to form Si−Si bonds. The octanol molecules subsequently displace the phenyl groups and cap the Si particle surface.

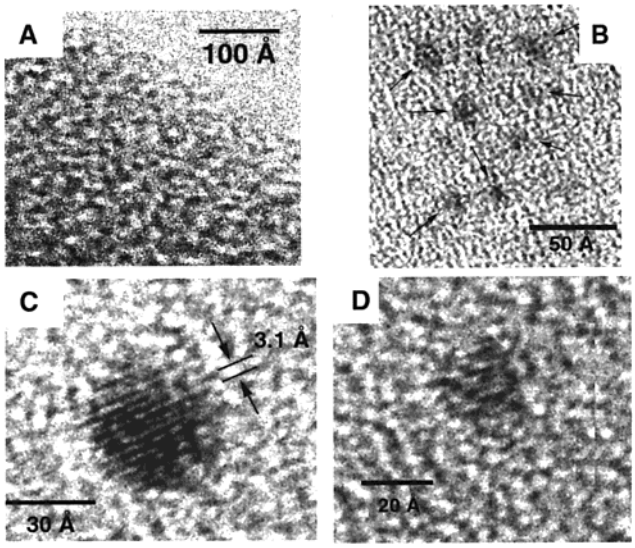

Figure 5. TEM images of Si nanocrystals: (A) Low-resolution TEM image of an aggregate of 15 Å diameter Si nanocrystals extended out from the edge of a carbon film. EDS of the aggregate (Figure 6) confirmed that the nanocrystals were Si. (B) High-resolution TEM image of several 15 Å diameter Si nanocrystals. (C and D) High-resolution images of 35 and 25 Å diameter sterically stabilized Si nanocrystals. The lattice planes are visible in the 25 Å diameter nanocrystals.

Size-monodisperse 15 Å diameter Si nanocrystals were obtained by reacting diphenylsilane in pure octanol with subsequent redispersion in ethanol. A fraction of the sample is made up of larger Si nanocrystals that form during the reaction that do not resuspend in ethanol due to their hydrophobicity, whereas the extreme surface curvature of the 15 Å diameter nanocrystals provides ethanol with "access" to the polar Si−O−C capping layer termination to enable the size-selective dispersion of 15 Å diameter Si nanocrystals. The 15 Å diameter nanocrystals are barely perceptible in TEM images obtained with samples dispersed on a carbon-coated TEM grid (Figure 5). In Figure 5A, a low-resolution image of an aggregate of these 15 Å diameter nanocrystals also shows that the sample contains little size variation. For comparison, TEM images in Figure 5 of larger Si nanocrystals with diameters ranging from 25 to 35 Å produced by performing the synthesis in sc-hexane with increased Si:octanol mole ratios clearly reveal highly crystalline cores and faceted surfaces. Crystalline lattice planes are observed in nanocrystals as small as 25 Å. Electron diffraction from these nanocrystals (Figure 6) also confirms that the nanocrystals consist of crystalline Si cores with diamond lattice structure.

A variety of other techniques were used to characterize the Si nanocrystals, including energy-dispersive X-ray spectroscopy (EDS), X-ray photoelectron spectroscopy (XPS), Fourier transform infrared spectroscopy (FTIR), UV−vis absorbance, and PL and PLE spectroscopy. In situ EDS measurements, shown in Figure 7, of the nanocrystals imaged by TEM revealed Si in high abundance with the presence of oxygen and carbon as well. A quantitative analysis of the elemental ratios was not possible since the supporting substrate was carbon containing a measurable amount of residual oxygen. XPS, however, provides an elemental analysis of the particles which gives an indication of how the nanocrystals are capped with the organic ligands.

Figure 8 shows XPS data for 15 Å diameter Si nanocrystals, which reveals that the sample contains a Si:C ratio of 0.70:1.

(17) March, J. *Advanced Organic Chemistry: Reactions, Mechanisms, and Structure*, 4th ed.; Wiley: New York, 1992.

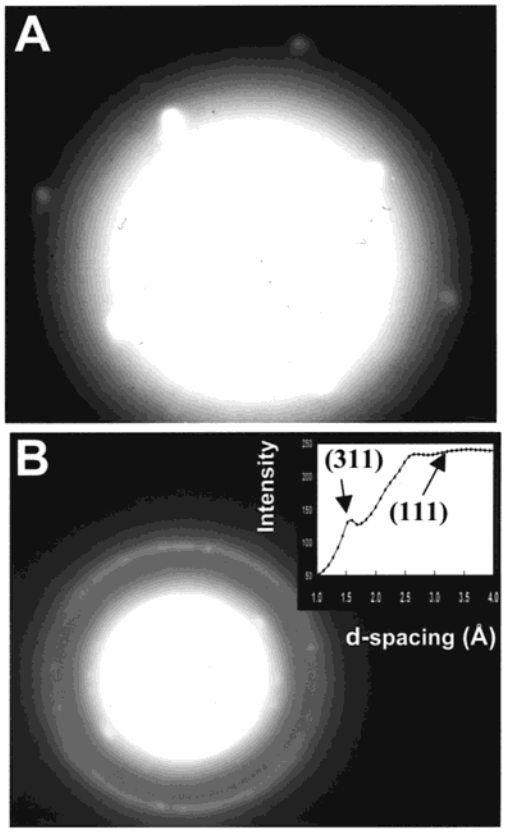

Figure 6. Electron diffraction images and data for Si nanocrystals: (A) Diffraction pattern from a few Si nanocrystals with (200), (400), and (511) orientation. (B) Diffraction of many Si nanocrystals predominantly (111) and (311) oriented (Inset: measured *d* spacings of 1.6 and 3.2 Å correspond to the (311) and (111) lattice spacings in Si).

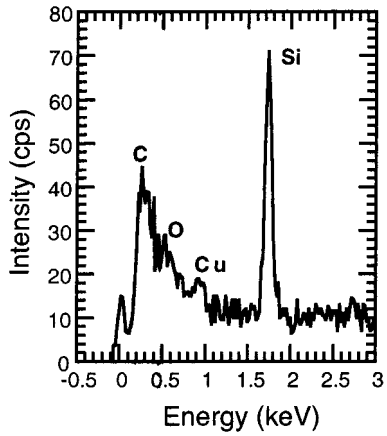

Figure 7. EDS data of the nanocrystals imaged by TEM in Figure 4A. The copper peak results from the copper TEM grid used as the material support.

By using a shell approximation, $d_p = a_{Si}(3N_{Si}/4\pi)^{1/3}$, where a_{Si} is the lattice constant (5.43 Å), the number of Si atoms, N_{Si}, in a nanocrystal can be calculated. Particles with 15 Å diameter (d_p) have approximately 88 atoms. The Si:C ratio determined from XPS can be used to calculate approximately the area occupied on the nanocrystal surface by each capping ligand. With the Si:C ratio equal to 0.7, the 15 Å cluster with 88 core Si atoms has 125 C atoms surrounding it. Each ligand has 8 carbons. Therefore, each particle is surrounded by approximately 16 capping ligands. Dividing the particle surface area by 16 indicates that each ligand occupies an average of 44 Å^2. This

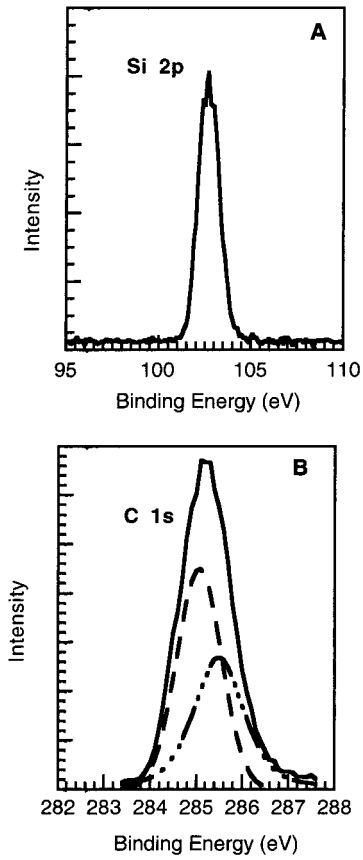

Figure 8. XPS of the 15 Å diameter Si nanocrystals deposited on a graphite substrate: (A) Si 2p region in the spectrum (modified area is 592.2 counts) and (B) C 1s region (−) and its deconvoluted peaks from the graphite substrate (− −) and the capping ligand (− ··· −). The modified area of the C 1s curve due to the capping ligand is 850.5 counts. The silicon-to-carbon ratio (Si:C) is 0.70:1.

value is about twice that expected for a close-packed monolayer of ligands surrounding the nanocrystals. Therefore, XPS indicates that the ligands coat the nanocrystals with approximately 50% surface coverage. An estimate of the surface coverage of the largerst 20 Å diameter nanocrystals in the sample size distribution gives an area per molecule of 33 Å^2, for approximately 70% surface coverage.

FTIR spectra show that the nanocrystals are most likely terminated with a combination of hydrogen and hydrocarbon chains, bound through an alkoxide (Si−O−C) linkage. In Figure 9, the four characteristic methylene and terminal methyl stretching modes $\tilde{\nu}_{a(CH_2)} = 2928$ cm^{-1}, $\tilde{\nu}_{s(CH_2)} = 2855$ cm^{-1}, $\tilde{\nu}_{a(CH_3,ip)} = 2954.5$ cm^{-1}, $\tilde{\nu}_{s(CH_2,FR)} = 2871$ cm^{-1}, reveal that a hydrocarbon steric layer has indeed adsorbed to the particle surface. The notable absence of the hydroxyl stretch ($\tilde{\nu}_{(O-H)} = 3300$ cm^{-1}) and the presence of the strong doublet corresponding to the Si−O−CH_2− stretching modes, $\tilde{\nu}_{(Si-O-CH_2-)} = 1100-1070$ cm^{-1}, suggests covalent alkoxide bonding to the Si nanocrystal surface.[18] Siloxane Si−O−Si stretches typically occur at slightly lower wavenumber (1085 and 1020 cm^{-1}); however, the presence of residual oxide on the nanocrystal surfaces cannot be completely excluded based on these data alone. The absence of the very strong characteristic aryl−Si stretching mode, at $\tilde{\nu}_{(Si-Ph)} = 1125-1090$ cm^{-1}, confirms precursor degradation. The lack of the strong $\tilde{\nu}_{(Si-C-Si)} = 1080-$

(18) Pretsch, E.; Clerc, T.; Seibl, J.: Simon, W. *Tables of Spectral Data for Structure Determination of Organic Compounds*: Springer-Verlag: Berlin, 1942. Socrates, G. *Infrared Characteristic Group Frequencies Tables and Charts*; John Wiley & Sons: New York, 1994.

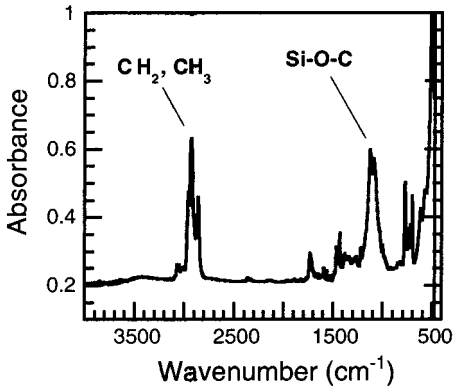

Figure 9. FTIR spectrum of Si nanocrystals on a ZnSe window. The spectrum reveals that the sterically stabilizing hydrocarbon chains are covalently linked to the Si surface through alkoxide linkages. These covalent linkages give rise to highly stable optical properties in the presence of ambient oxygen and water.

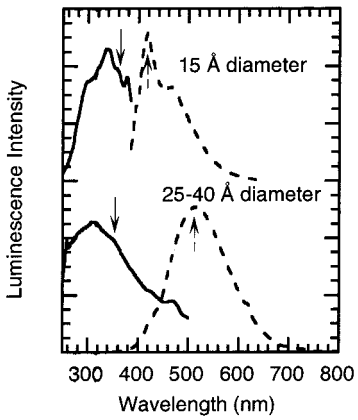

Figure 10. Room-temperature PL (solid lines, excitation energy denoted by solid arrows) and PLE (dashed lines, detection energy denoted by dashed arrows) spectra of Si nanocrystals. The spectra of 15 Å diameter nanocrystals are compared with spectra of slightly larger particles with a broader size distribution.

1040 cm^{-1} stretching mode eliminates the possibility that the nanoparticles consist of a Si−C core, or that the alkane layer is directly adsorbed to the Si surface. Strong Si TO (transverse optical) phonon bands occur between 450 and 520 cm^{-1}, indicating that the particles are composed of Si only.[19,20] Strong peaks between 750 and 850 cm^{-1} and subtle absorption peaks in the range 2100 to 2300 cm^{-1} can possibly be assigned to a variety of Si−H stretching modes.[18] There is also a possible carbonyl stretch at $\tilde{\nu} \cong 1700$ cm^{-1} that could result from octanol adsorption through a Si−C═O linkage if alcohol oxidation to the aldehyde occurs. On the basis of XPS and FTIR data, the nanocrystal surface is coated mostly by the hydrocarbon ligands. However, the remaining 30% to 50% of the surface is coated with a combination of hydrogen, Si−C═O, and possibly a small portion of oxide.

Optical Properties. The Si nanocrystals photoluminesce as shown in Figure 10 with overall quantum yields as high as 23% at room temperature. Several closely spaced discrete features

(19) The TO stretching modes occur at 517, 463, and 494 cm^{-1} for the Γ, X, and L critical points for bulk Si, respectively: Giannozzi, P.; de Gironcoli, S.; Pavone, P.; Baroni, S. *Phys. Rev. B* **1991**, *43*, 7231. These peak assignments, however, cannot be made unequivocally because of the possible presence of aromatic hydrocarbon impurities in the sample, which absorb in this frequency range.[18]

(20) A sharp IR absorbance peak occurs at 480 cm^{-1}, which may correspond to localized TO phonons: Scholten, A. J.; Akimov, A. V.; Dijkhuis, J. I. *Phys. Rev. B* **1993**, *47*, 13910.

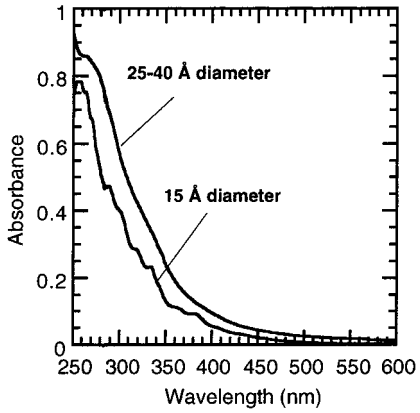

Figure 11. Room-temperature absorbance spectra of Si nanocrystals formed under supercritical conditions in the presence of octanol. The absorbance spectra were insensitive to solvent polarity, indicating that the absorbance is due to an exciton state and not a charge-transfer transition between bound ligands. Note the blue shift in the absorbance edge, and the appearance of discrete optical transitions in the spectra of the 15 Å diameter nanocrystals compared to the larger, more polydisperse nanocrystals.

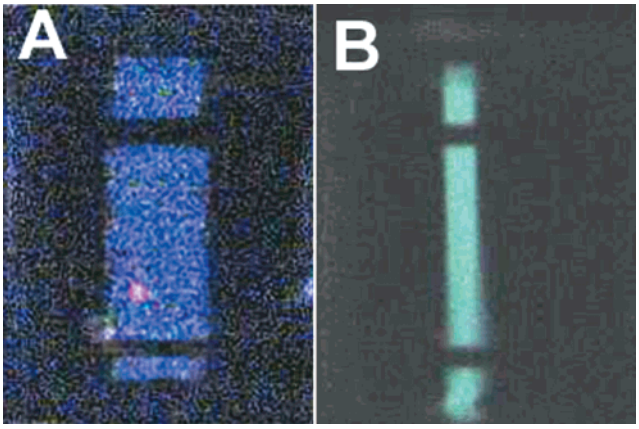

Figure 12. Photographic image of the luminescent Si nanocrystals excited at 320 nm in hexane: (A) 15 Å diameter Si nanocrystals and (B) 25−40 Å diameter nanocrystals. The smaller nanocrystals emit in the near-UV and appear deep blue, whereas the larger particles appear blue-green.

appear in the PLE spectra of the 15 Å diameter nanocrystals, which are mirrored by a few meV in the absorbance spectra in Figure 11. As shown in Figure 10, the nanocrystals exhibit size-dependent PL and PLE spectra, with the smaller nanocrystals (15 Å diameter) emitting in the near-UV and the larger nanocrystals (25 to 40 Å diameter) emitting green light (see Figure 12). For all sizes, the absorption coefficient α, was found to increase quadratically with incident energy, $\alpha \sim [h\nu - E_g]^2$, near the absorption edge (Figure 13), which is characteristic of a predominantly indirect transition.[9] Figure 13 compares the extinction coefficients for bulk Si with those measured for the 15 Å diameter nanocrystals. The indirect $\Gamma \rightarrow X$ transition remains the lowest energy transition, increasing from 1.2 eV (bulk Si) to 1.9 eV due to quantum confinement. It should be noted that it appears that the direct $\Gamma \rightarrow \Gamma$ transition has *red* shifted to 3.2 eV from 3.4 eV and the $L \rightarrow L$ transition energy has blue-shifted from 4.4 eV to 4.7 eV, in *quantitative* agreement with empirical pseudopotential calculations by Ramakrishna and Friesner,[21] although these assignments cannot be made conclusively. Further comparison of the extinction coefficients measured for the nanocrystals with values for bulk

(21) Ramakrishna, M. V.; Friesner, R. A. *J. Chem. Phys*. **1992**, *96*, 873.

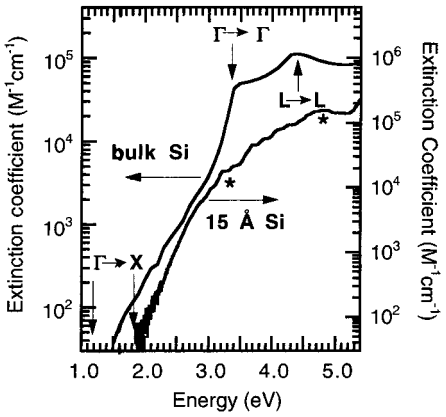

Figure 13. Extinction coefficients plotted on a log scale for bulk Si and those measured for 15 Å Si nanocrystals formed by arrested precipitation in supercritical octanol. The absorption edge corresponds to the indirect $\Gamma \rightarrow X$ transition and the two peaks in the bulk Si spectra correspond to the $\Gamma \rightarrow \Gamma$ and $L \rightarrow L$ critical points at 3.4 and 4.3 eV, respectively. Note the apparent blue shift of the $\Gamma \rightarrow X$ and $L \rightarrow L$ transitions in the nanocrystals due to quantum confinement and the apparent red shift of the $\Gamma \rightarrow \Gamma$ transition, as predicted by Ramakrishna and Friesner in ref 21.

Si reveals an overall lifting of the critical point degeneracies (direct transitions at $k = 0$ and away from $k = 0$), as predicted by both empirical pseudopotential[21] and tight-binding[22] calculations, and an oscillator strength enhancement. These results contrast the spectra for slightly larger, more polydisperse Si nanocrystals, ranging in size from 25 to 40 Å in diameter in Figure 11, which exhibit monotonically increasing featureless absorbance spectra. A slight exciton peak, however, does seem to appear in the PLE spectra in Figure 10 for the larger nanocrystals at 2.6 eV (470 nm).

The Si nanocrystal PL was remarkably stable in the presence of atmospheric oxygen, especially when considering the sensitivity of the optical properties of porous-Si to surface chemistry, such as oxidation.[12,23] The sc-technique provides Si nanocrystals with sufficiently robust surface passivation to prevent strong interactions between the Si cores and the surrounding solvent to enable efficient luminescence from Si. Comparison between the PL and PLE spectra in Figure 10 reveals a Stokes shift of approximately 100 meV with respect to the lowest energy peak in the PLE spectra. The relatively broad PL peak has a characteristic lifetime of 2 ns, indicating that various nonradiative processes are important in the nanocrystals. It is worth noting that the low-energy PL peak observed by Brus et al.[4] for ~20 Å diameter oxide-coated Si nanocrystals at 1.6 eV was not observed in any of these samples.

The origin of the photoluminescence in Si nanocrystals is quite complex and remains actively debated. The PL spectrum in Figure 10 is clearly size dependent, with the larger particles emitting lower energy light than the smaller particles, consistent with the general perception of quantum confinement effects in Si. The PL from Si nanocrystals, however, has been shown to be highly sensitive to surface chemistry, especially the presence of oxide on the nanocrystal surface.[12,23] Indeed, the PL spectrum of the 15 Å diameter nanocrystals is complicated by the presence of two prominent peaks in the 15 Å nanocrystal spectrum as shown in Figure 10: one at 2.95 eV (419 nm) and one at 2.65 eV (467 nm). Furthermore, the PL was found to depend on the excitation wavelength, with 3.4 eV (363 nm) excitation yielding the highest quantum yield and the sharpest PL. Increasing the excitation energy from 3.4 eV to 4.4 eV (281 nm) led to a decrease in the intensity of the highest energy feature with respect to the low-energy "satellite" peak, and a decrease in the overall quantum yield. Although we cannot assign these peaks conclusively at this time, we propose that the higher energy peak is intrinsic to quantum confinement in Si nanocrystals and the lower energy peak results from the presence of oxygen on the particle surface, as proposed in ref 12 for porous Si. Wolkin et al.[12] calculated that the PL energy due to intrinsic quantum confinement in Si can in some cases differ from the PL energy due to surface states, specifically Si═O. For nanocrystals greater than 3 nm in diameter, the intrinsic and surface state emission energies are the same, with emission at 2 eV (620 nm).[12] However, 15 Å diamater nanocrystals were predicted to give rise to intrinsic PL at 2.8 eV, and surface state PL resulting from the presence of oxygen at 2.3 eV (537 nm).[12] The PL spectra of the Si nanocrystals shown in Figure 10 are consistent with this interpretation. It should be noted, however, that peak splitting due to separate direct and phonon-assisted absorption and emission events has been observed by Calcott et al.[24] for porous Si and may provide an alternative explanation.

Conclusions

Sc-octanol serves as an effective capping ligand for the synthesis of Si nanocrystals. Significant quantities of stable, well-passivated nanocrystals can be produced in a simple batch reactor. The smallest size-monodisperse 15 Å diameter Si nanocrystals exhibit previously unobserved discrete electronic absorption and luminescence transitions due to quantum confinement effects. This study also confirms that Si clusters as small as 15 Å in diameter still behave as indirect semiconductors. This supercritical route for nanostructure formation might be applied to other materials, such as Si nanowires,[25] that require high temperatures for crystal formation and the solvation of capping ligands.

Acknowledgment. B.A.K. thanks the Welch Foundation, the National Science Foundation, and DuPont for support. K.P.J. thanks the Department of Energy and the National Science Foundation for support.

JA002956F

(22) Hill, N. A.; Whaley, K. B. *Phys. Rev. Lett*. **1995**, *75*, 1130. Hill, N. A.; Whaley, K. B. *J. Electron. Mater*. **1996**, *25*, 269.
(23) Lauerhaas, J. M.; Sailor, M. J. *Science* **1993**, *261*, 1567.
(24) Calcott, P. D. J.; Nash, K. J.; Canham, L. T.; Kane, M. J.; Brumhead, D. *J. Phys.: Condens. Matter* **1993**, *5*, L91.
(25) Holmes, J. D.; Johnston, K. P.; Doty, R. C.; Korgel, B. A. *Science* **2000**, *287*, 1471.